One-dimensional single-crystalline Ti–O based nanostructures: properties, synthesis, modifications and applications

Weijia Zhou,[a] Hong Liu,*[a] Robert I. Boughton,*[b] Guojun Du,[a] Jianjian Lin,[c] Jiyang Wang[a] and Duo Liu[a]

Received 4th January 2010, Accepted 4th March 2010
DOI: 10.1039/b927224k

Recent advances in the properties, synthesis, modifications and applications of one-dimensional single-crystalline Ti–O based nanostructures (including nanotubes, nanobelts, nanowires, and nanorods) are reviewed. The physical and chemical properties of one-dimensional nanostructured titanates, such as adsorption, stability, ion-exchange, optical, and proton conductivity properties, are described in connection with a particular application. The experimental parameters, morphologies, and mechanism of formation of one-dimensional nanostructured titanates produced by the alkaline hydrothermal method are critically discussed. Current progress in the modifications of one-dimensional single-crystalline Ti–O based nanostructures are discussed together with their improved performances. Examples of applications of one-dimensional nanostructured titanates in photocatalysis, lithium batteries, sensors, hydrogen production and storage, solar cells and biomedicine are presented.

1. Introduction

Much recent research has focused on controlling the size, shape, crystal structure and surface properties of semiconducting oxide nanomaterials in order to tailor them for a particular application. Their physical and chemical properties can often be significantly different from those of the corresponding bulk materials. Iijima discovered fullerene-related carbon nanotubes in 1991, which attracted wide attention to investigating one-dimensional nanomaterials.[1] Over the past decade, one-dimensional (1D) semiconducting oxide nanostructures (ZnO, SnO_2, In_2O_3, Ga_2O_3, V_2O_5), such as nanotubes (NTs),[2,3] nanobelts (NBs),[4–6] nanowires (NWs)[7–9] and nanorods (NRs)[10] have attracted extraordinary attention due largely to the unique physical and chemical properties associated with the 1D structural confinement at this scale. Titanium dioxide (TiO_2) is an exceptional material that has many promising applications in areas ranging from pigments and toothpaste,[11,12] to photocatalysis,[13,14] solar cells[15,16] and sensors.[17–19] Recently, titanate nanotubes,[20] nanobelts,[21] nanowires[22] and nanorods,[23] have received much attention because of the wide applications and relatively simple preparation procedures needed to fulfill the requirements of various applications. One-dimensional single-crystalline Ti–O based nanomaterials have properties that compare with nanoparticle titania but possess a high surface-to-volume ratio as well. Among some of the unique properties, the movement of electrons and holes in TiO_2 semiconductor nanomaterials is primarily governed by quantum confinement, and the transport

[a]*State Key Laboratory of Crystal Materials, Center of Bio & Micro/nano Functional Materials, Shandong University, 27 Shandanan Road, Jinan, 250100, China. E-mail: hongliu@sdu.edu.cn*
[b]*Department of Physics and Astronomy, Green State University, Bowling Green, OH, 43403, USA. E-mail: boughton@bgnet.bgsu.edu*
[c]*Department of Materials Science and Engineering, Shandong Institute of Light Industry, Jinan, 250353, China*

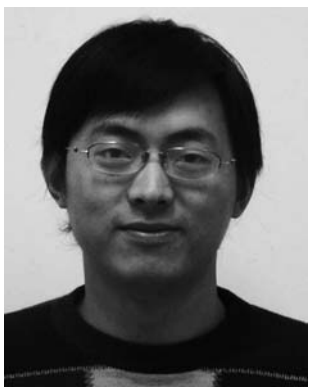

Weijia Zhou

Weijia Zhou obtained his M.Sc. from Shandong Institute of Light Industry, China, in 2009. Currently he is pursuing his Ph.D. degree under the supervision of Prof. Hong Liu and Prof. Jiyang Wang in State Key Laboratory of Crystal Materials, Shandong University, China. His research interest in his Ph.D. study is mainly focused on the preparation and modifications of one-dimensional Ti–O based nanomaterials for photocatalysis applications.

Hong Liu

Dr Hong Liu received his B.Sc degree from Shandong Institute of Light Industry in 1985, and his Ph.D. degree from Shandong University in 2001. He is a professor in State Key Laboratory of Crystal Materials, Shandong University, China. His research interests are related to synthesis of nanomaterials, the application of nanomaterials in gas and biosensors, environmental protection, and new energy sources.

properties related to electrons and photons are largely affected by their one-dimensional geometry.[24]

Over the past few years, many methods have been developed for the successful fabrication of one-dimensional TiO_2 nanomaterials, including the hydrothermal method,[25–29] the sol–gel method,[30] template-based synthetic approaches[31,32] and electrochemical synthesis.[33,34] However, for one-dimensional single-crystalline Ti–O based nanostructures, hydrothermal synthesis appears to be the most effective method. Kasuga *et al.*[35] first discovered the alkaline hydrothermal route for titanium oxide synthesis with a tubular shape, which caused a great deal of interest. Recently, many researchers have explored different approaches to modifying one-dimensional TiO_2 semiconductors by assembling a variety of noble metals quantum dots and semiconductors nanostructures on the surface of the one-dimensional TiO_2 nanomaterials.[36–40] Investigators have measured more efficient electron diffusion in these single-crystalline nanomaterials. The properties of one-dimensional nanostructures, with their high specific surface area and novel semiconducting properties, make nanostructured titanates and TiO_2 promising for many applications, including photocatalysis, lithium batteries, sensing applications, hydrogen production and storage, solar cells and biomedical applications.

In recent years, breakthroughs have continually been made in the preparation, modification, and applications of TiO_2 nanomaterials and other one-dimensional semiconductor oxide nanostructures. Several excellent reviews of the subject exist in the literature.[41–45] Nevertheless, we believe that a new and comprehensive review of one-dimensional single-crystalline Ti–O based nanomaterials would further promote the corresponding research and development efforts to open a wider area for the applications. In this review, single-crystalline one-dimensional Ti–O based nanostructures are the focus. Comparison of structure, properties, preparation, modifications and applications of different one-dimensional single-crystalline Ti–O based materials, including titanate, titanic hydroxide, and TiO_2, are summarized. The hydrothermal experimental conditions and synthesis mechanisms for fabricating different one-dimensional titanate nanostructures are considered. Modifications of one-dimensional TiO_2 nanostructures to obtain specific physical excellent properties are discussed and examined. Analysis of the physical and chemical properties of single-crystalline Ti–O based titanates and recent progress in their applications allow for the identification of gaps in our knowledge and highlight the need for critical studies in the area of nanostructured titanates.

2. Structure and properties

2.1 Structure

Titania exists naturally in three crystalline polymorphs, namely rutile (3.05 eV), anatase (3.23 eV), and brookite (3.26 eV). Rutile is the most common and stable TiO_2 polymorph. Both rutile and anatase have a tetragonal structure with $a = 0.459$ nm and $c = 0.296$ nm (rutile); $a = 0.536$ nm and $c = 0.953$ nm (anatase). Brookite has an orthorhombic structure with $a = 0.915$ nm, $b = 0.544$ nm, and $c = 0.514$ nm. TiO_2 is known as an n-type semiconductor, which contains donor-type defects such as oxygen vacancies and titanium interstitials. Identification of the crystal structures of one-dimensional single-crystalline Ti–O based nanomaterials has given rise to much debate in the recent literature.[46,47] Ti–O based nanotubes are thought to be caused by scrolling of an exfoliated TiO_2-derived nanosheet into a hollow multiwall nanotube with spiral cross section. Unlike carbon nanotubes produced by the catalytic pyrolysis of hydrocarbons, titania nanotubes produced *via* the alkaline hydrothermal method have never been observed in single layer form. All reports of TiO_2 nanotubes describe the samples as multilayer-walled nanotubular structures. The number of layers varies from two to ten. They are open-ended with several wall layers on both sides. The layered TiO_2 structures can be described as stacked polyanion sheets of interconnected MO_6^{n-} octahedra with intercalated cations in the interlayer region.[48]

Up to now, several possible crystal structures of nanotubular products from the alkaline hydrothermal treatment of TiO_2 have been proposed, including hydrogen titanate $H_2Ti_3O_7$,[28,49] $Na_xH_{2-x}Ti_3O_7$ ($x = 0.75$),[50] orthorhombic titanates $Na_2Ti_2O_4(OH)_2$[51] and tetratitanates $H_2Ti_4O_9$.[52] Nanobelts, nanowires and nanorods structures tend to have good crystallinity and usually the relation between the length of the edges corresponding to each crystallographic axis is arranged in the order (001) ≫ (100) ≫ (010). The length of nanowires (001) can

Robert I. Boughton

Dr Robert I. Boughton is a Professor and Chair at Department of Physics and Astronomy at Bowling Green State University at Bowling Green. He obtained his Ph.D. degree in physics from Ohio State University in 1968. His current research involves low temperature electrical, magnetic and thermoelectric properties of pure metals and superconductors; numerical simulation of electron transport properties in metals; and physics education.

Jiyang Wang

Mr Jiyang Wang is a Professor, of State Key Laboratory of Crystal Materials, at Shandong University, China. His research interests focus on the research of functional single crystal growth, property and its application, especially for laser and nonlinear optical crystals. He has published more than 200 papers on international journals, and 30 patents.

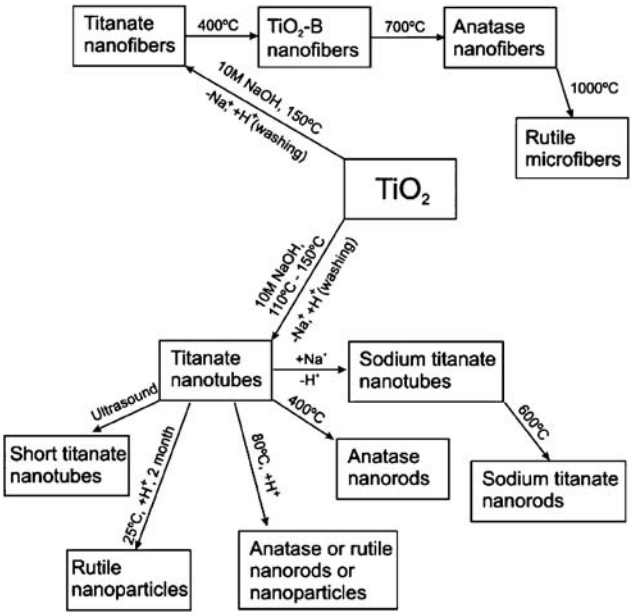

Fig. 1 Scheme of transformation of one-dimensional single-crystalline Ti–O based nanostructures.[54]

be several tens of micrometres, while the width (100 or 010) is typically in the range of 10–100 nm. Tafen and Lewis[53] studied nanowires with a [001] growth direction having several perimeter and surface-facet configurations. For each nanowire, the atomic structure was carved out from the anatase phase of TiO_2. The mutual transformation among the titanate nanotubes, nanobelts, nanowires and nanorods can be made under certain condition and the generalized scheme is shown in Fig. 1.

The precise crystal structures of one-dimensional single-crystalline Ti–O based nanomatersials is still an open question because of several intrinsic difficulties posed by the specific nanostructures. First, both the small crystallite size of one-dimensional nanostructures and their wrapping along specific crystallographic axis results in a broadening of the diffraction lines. Second, there are a large number of crystal modifications not only for pure TiO_2 (anatase, rutile, and brookite) but also for the protonated forms of polytitanic acids, $H_{2m}Ti_nO_{2n+m}$. Through X-ray diffraction, Raman, X-ray absorption fine structure, and electron diffraction measurements, Ma *et al.*[46] found that both nanotubes and nanobelts may have a layered titanate origin. Extended X-ray absorption fine structure (EXAFS) analysis has demonstrated that the three-dimensional structure of "TiO_2-type" nanotubular materials produced by the alkaline hydrothermal method can be interpreted as an arrangement of TiO_6 octahedrons in corrugated layers.[55] Fourier transform infrared (FTIR) spectra of the nanotubes/nanobelts show very similar peak positions and profiles to those exhibited by protonic lepidocrocite titanate.

2.2 Properties

A more recent approach has been in the synthesis of one-dimensional titanium oxide in the form of nanotubes, nanowires, nanobelts and nanorods with the view that dimensional confinement in combination with novel shapes will reveal interesting physical and electrical properties.[56,57] Although the energy gap of these single-crystalline nanostructural titania shows little alteration compared with bulk TiO_2, they do display an increase in photoactivity due to better charge transport in the crystallites, higher surface defect content, and an inherently higher aspect ratio.[58–60] Moreover, the size and shape of nanocrystalline semiconductors are known to be important factors in influencing the nature of the bonding and packing density of sensitizing molecules and compounds. These features have a significant impact on the charge-transfer process from the sensitizer to the semiconductor. The exotic surface geometry that these nanostructural titania possess make them excellent candidates to explore such factors.

2.2.1 Adsorption properties. The one-dimensional titanium oxides have a large surface area (see Table 1), which facilitates reaction/interaction between the devices and interacting

Table 1 The surface area S_{BET} of one-dimensional titanium oxide with different morphologies

Synthetic conditions	Formula	Morphologies	BET/m^2 g^{-1}	Ref.
Hydrothermal treatment at 130 °C for 24 h	TiO_2	Nanotubes: the tube size ranges between 10 and 30 nm	400	61
Hydrothermal treatment at 107 °C for 48 h and acidic treatment	$H_2Ti_3O_7$	Nanotubes: scrolled up hollow structures with inner diameter of 4 nm, outer diameter of 12 nm, and lengths of about 100 nm	280	62
Hydrothermal treatment at 107 °C for 48 h	$Na_2Ti_3O_7$	Nanowires: widths of about 50–100 nm and lengths up to micrometres	130	62
Hydrothermal treatment at 180 °C for 24 h and annealed at different temperatures	TiO_2	Nanobelts: the mesoporous nanobelts with the average pore size of 9.07 nm and smooth surface	38.0 and 27.7	63
Hydrothermal treatment at 200 °C for 36 h and HNO_3 post-treatment at 180 °C for 24 h, pH = 7	$H_2Ti_3O_7$ and TiO_2	$H_2Ti_3O_7$ nanofibers: 40–300 nm in thickness, tens of micrometres in length; TiO_2 nanorods: porous rod-like structure	34.1 and 47.0	64
Hydrothermal treatment at 200 °C for 48 h and hydrothermal post-treatment at 150 °C for 24 h.	$H_2Ti_3O_7$ and TiO_2	Belt-like structure for $H_2Ti_3O_7$ and rod-like morphology for TiO_2	18.3 and 61.6	66

media,[61–64] which mainly occurs on the surface or at the interface. One-dimensional titanium oxide with a large surface area can be used as catalytic carrier and be beneficial in absorbing degradation products. Umek[65] reported that the active surface area for nanotubes (at 115 and 135 °C) ranges from 200 to 240 $m^2 g^{-1}$, while for nanoribbons (at 175 and 195 °C) it is only about 30 $m^2 g^{-1}$. Using the titania nanotubes and nanoribbons as adsorbents for NO_x was investigated. When exposed to NO_2 gas, NO_2 molecules tend to physisorb onto the nanotube surface *via* the nonbonding π orbital of the oxygen atoms. The results show that the catalysis difference between nanotubes and nanoribbons can be attributed to their surface morphology and the amount of active surface area, which in certain cases allows for catalytic reactions of the NO_2 molecules on the titania-based surface.

2.2.2 Stability properties. Titanate nanotubes have poor stability in dilute inorganic acids even at room temperature, and slowly transform to rutile nanoparticles over several months. The rate of transformation depends on the nature of the inorganic acid and is correlated to the solubility of the titanates in the acid. Acidic hydrothermal treatment of titanate nanotubes at 175 °C[67] or hydrothermal conditions even in the absence of acid[68,69] results in the formation of polycrystalline nanostructured anatase structures, such as nanorods. Bavykin *et al.*[70] reported the nanotubes were stable and minimal morphological changes occurred in pure water and basic (0.1 mol dm^{-3} NaOH) solutions. In 0.1 mol dm^{-3} H_2SO_4, suspended titanate nanotubes slowly transform to rutile nanoparticles of *ca.* 3 nm size, which agglomerated into ellipsoidal particles. In 0.1 mol dm^{-3} solutions of HCl and HNO_3 the process of transformation is several times slower and the concentration of soluble Ti^{4+} is also several times lower than in 0.1 mol dm^{-3} H_2SO_4, confirming that the mechanism of acid-assisted transformation includes the dissolution of nanotubes, release of soluble forms of Ti^{4+} in solution, and crystallization of dissolved Ti^{4+} into rutile nanoparticles.

Physically, titanate nanotubes are relatively fragile and can be easily broken up by mechanical forces during ultrasonic treatment, resulting in shorter nanotubes.[71] In addition, the nanotubes are not stable at high temperature. $H_2Ti_3O_7$ nanotubes are susceptible to lattice oxygen depletion and transform above 397 °C into complete rod-like structures. Recent systematic thermal transformation studies of titanate nanotubes[72,73] have revealed that annealing them in the temperature range 120–400 °C results in slow dehydration of the initial nanotubular $H_2Ti_3O_7$ to form nanotubular TiO_2(B) accompanied by a decrease in interlayer spacing of the nanotube walls. A further increase in temperature results in the transformation of nanotubular TiO_2(B) to anatase nanorods, which is accompanied by a loss of tubular morphology. Nanofiber titanates can transform to nanofibrous TiO_2(B) at 400 °C, followed by transformation to nanofibrous anatase at 700 °C and then completely transformed to submicron rod-like structure of rutile at 1000 °C.[74] The formation of anatase nanofibers is also possible by using hydrothermal post-treatment of the titanate nanofibers in water at 150 °C.[66] Compared with nanotubes, Riss *et al.*[62] found that nanowires have higher thermal stability, and retain their structure and morphology over the entire temperature range of 197 to 597 °C.

The role of Na ions in titante nanotubes (TNTs) was investigated by Suetake *et al.*[75] There exist two Na ion states in the TNTs, strongly and weakly interacting with the TNT system. The Na ions that are strongly bound in the TNT interlayer play an important role in stabilizing the tube structure. The thermal stability and nature of thermal transformations during annealing can be affected by the level of ion-exchanged sodium in nanotubular titanates.[76,77] When fully saturated with sodium ions, titanate nanotubes lose their nanotubular morphology and convert to $Na_2Ti_6O_{13}$ nanorods at 600 °C.[78] On the other hand, Na ions that interact weakly with the TNT surface suppress photocatalytic activity but can easily be removed by a weak acid treatment to lead to optimum photocatalytic activity.[75]

2.2.3 Ion-exchange properties. In the structure of one-dimensional single-crystalline Ti–O based nanostructures, protons occupy the cavities between the layers of the TiO_6 octahedra. The open morphology of the nanotubes results in effective ion-exchange properties. Ion-exchange reactions were carried out in aqueous ammonia solution with alkaline ions (Li^+, Na^+, K^+, Rb^+, Cs^+)[79] and some transition-metal ions (Co^{2+}, Ni^{2+}, Cu^{2+}, Zn^{2+}, Cd^{2+})[50] placed between the layers of multilayered nanotubes. However, they do not affect the interlayer distance, indicating that the rigidity of the titanate framework is maintained during ion exchange. The ions exchange with the titanate framework *via* electrostatic interactions between the negatively charged host lattice and the positively charged cations. It was found that when titanate is washed with dilute acid, sodium ions are substituted by protons and consequently reduce the electrostatic interaction between the titanate sheets. Sun and Li[50] and Kim and Cho[80] found that the specific surface area of nanotubes and nanowires can be increased by ion exchange. The BET surface area of the original nanotubes was 99 $m^2 g^{-1}$, while that of Co-substituted titanate nanotubes had increased to 243 $m^2 g^{-1}$. Kim and Cho[80] reported that spinel $Li_4Ti_5O_{12}$ nanowires prepared by firing a mixture of $TiO_2 \cdot 1.25H_2O$ nanowires and Li acetates at 800 °C for 3 h have a superior rate capability even at a 10 C rate, retaining over 93% of the original capacity. These results were associated with a more active surface in the nanowires which facilitates faster lithium diffusion on account of shorter pathways. TiO_2 nanobelts can be doped with Co[81] and Ni[82] to obtain special magnetic properties. Zhang *et al.*[82] reported that Ni-doped TiO_2 samples exhibit complex magnetic properties including room-temperature ferromagnetic and paramagnetic behavior. With an increase of Ni^{2+} content, the magnetization also increases with the same applied field owing to the uniform distribution of Ni^{2+} ions in the TiO_2 nanobelts.

2.2.4 Optical properties. Titanate nanotubes are wide-bandgap semiconductor materials. As with aqueous colloids of titanate nanotubes at room temperature, the bandgap has been estimated to be *ca.* 3.87 eV,[83] which is very close to the bandgap of *ca.* 3.84 eV in 2D titanate nanosheets,[84] but much higher than the value of *ca.* 3.2 eV in bulk TiO_2. The absorption spectrum of titanate nanotubes coincides with luminescence transitions of single or multilayered titanate nanosheets demonstrating the apparent 2D behavior of the 1D tubes at room temperature. At the same time, changing the internal diameter of TiO_2 nanotubes over the range of 2.5–5 nm does not change the position of absorption and emission bands, which also demonstrates that two-dimensional optical properties dominate in TiO_2

nanotubes.[83] Zhang *et al.*[85] indicate that the optimal excitation wavelength for TiO_2 nanowires is 473 nm. The photoluminescence (PL) intensity of TiO_2 nanowires is higher than that of TiO_2 nanocrystals under all circumstances, which indicates that the nanowires might have a higher activity than nanocrystals. So, one can conclude that TiO_2 nanowires have a very strong photoluminescence band in the blue–green wavelength range.

2.2.5 Proton conductivity properties. Thorne *et al.*[73] found that TiO_2 nanotubes have high protonic conductivity. Conductivity measurements indicate that mainly protonic transport occurs at temperatures below 150 °C, and with increasing temperature, the progressive breakdown of nanotubes, and the formation of crystalline TiO_2 phases, results in the loss of protonic conductivity, leaving only residual electronic defect conduction. The proton conductivity is *ca.* 5.5×10^{-6}/S cm at 27 °C. The TNT electrode used in the dye-sensitized solar cells (DSSCs) has a longer electron lifetime, which results in an increase in electron density, leading to a high open-circuit voltage.[86] The $Na_2Ti_6O_{13}$ nanobelt is verified to be a semiconducting ceramic by Zhen, which has a electrical resistivity of about 3.86 Vm.[87]

3. Synthesis

3.1 Hydrothermal method

For the synthesis of single-crystalline Ti–O based nanostructures, the hydrothermal method has merited much attention due to its simple procedure and low production cost. Ever since high-quality, high-purity titania-based nanotubes were produced by using a simple hydrothermal treatment of TiO_2 powder in a NaOH aqueous solution by Kasuga *et al.*,[35,88] many investigations have been carried out on the formation of one-dimensional TiO_2 nanostructures. Recently, a mass of Ti–O based nanotubes,[17,89,90] nanobelts,[91] nanowires[92,93] and nanorods[77,94] produced by the hydrothermal method were reported, as shown in Fig. 2. Oriented arrays of titanium oxide nanotubes were successfully fabricated on a Ti foil seeded with TiO_2 nanoparticles in a hydrothermal procedure.[95] The outer surfaces may be negatively charged due to Ti vacancies, the same as with nanotubes that are scrolled up from $Ti_{0.91}O_2$ unilamellar nanosheets.[96] Li *et al.*[97] synthesized layered hydrogen titanate nanowires with uniform morphology from TiO_2 *via* an alkali hydrothermal process. In contrast to the scroll structure of hydrogen titanate nanotubes, nanowires have a layer-by-layer stacking structure. The average diameter of the as-prepared nanowires is about 100 nm with a uniform interlayer spacing of 0.81 nm. At the same time, the experimental parameters and synthesis mechanisms have been extensively researched.

3.1.1 Experimental parameters. It has been found that the hydrothermal temperature,[71] treatment duration,[98] starting materials[73,99] and base solution[100] have strong effects on controlling the morphology of the resulting product. As for the effect of the hydrothermal temperature and duration period on morphologies, many experiments have been carried out. Until recently, it was commonly accepted that nanotubes are formed under milder reaction conditions (130–150 °C and a time period between 24 and 72 h) by the rolling up of exfoliated trititanate crystal sheets. At a lower treatment temperature (lower than 120 °C), a large amount of residual TiO_2 particles can be found in the product. A higher temperature and longer duration (temperatures higher than 170 °C and 72 h to 1 week) promote unidirectional crystal growth, leading to nanowires, nanowhiskers or nanofibers.[100] To some extent, the synthesis temperature can control the average diameter of the nanotubes, as was reported by Bavykin.[71] Elsanousi *et al.*[98] have discussed the effect of the duration of the hydrothermal treatment on the

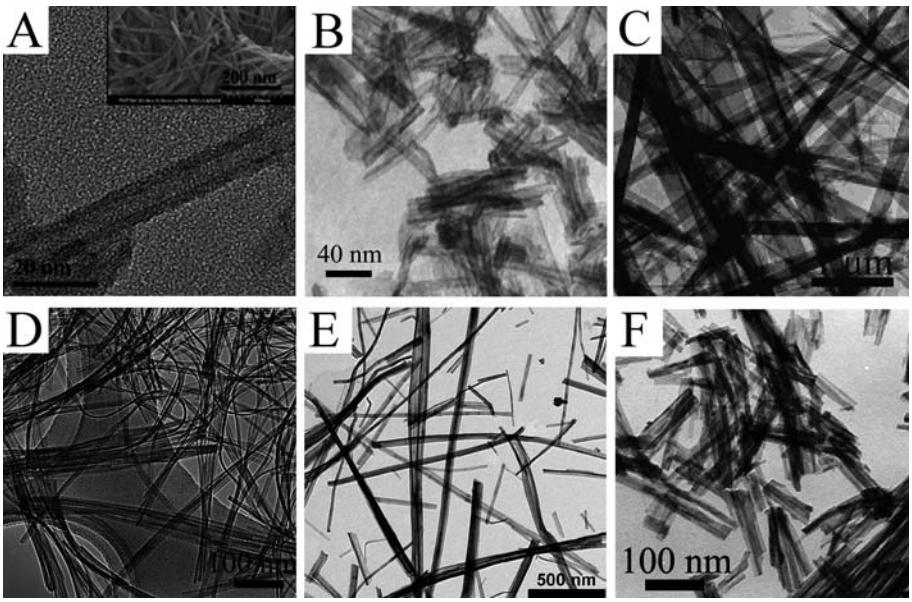

Fig. 2 Different morphologies of one-dimensional single-crystalline Ti–O based nanostructures: (A) TiO_2 nanotubes,[89] (B) $Na_2Ti_3O_7$ nanotubes,[90] (C) $Na_2Ti_3O_7$ nanobelts,[91] (D) $K_2Ti_8O_{17}$ nanobelts,[91] (E) $H_2Ti_3O_7$ nanowires[92] and (F) $Na_2Ti_3O_7$ nanorods.[94]

transformation of titanate nanotubes into nanoribbons at a specific hydrothermal temperature. At a fixed temperature of 180 °C, the morphology of the products transforms with a hydrothermal duration of 5 to 72 h. Hollow nanotubes with an outer diameter of about 10 nm were formed with a treatment duration of between 5 and 20 h at 180 °C. Bundles of nanoribbons with widths ranging from 50 to 500 nm and lengths of up to several tens of micrometres were produced with a duration of 72 h. Experimental results on samples treated at different temperatures (135–195 °C) for different durations reveal that the nanotubes transform into nanoribbons after a specific treatment duration at any temperature. At the same time, the synthesis time and temperature can be reduced or lowered by promoting one-dimensional titanate growth, with the use of microwave heating,[101,102] ultrasonication,[103] and a rotating autoclave[92] on the reaction mixture during synthesis.

The choice of initial raw materials may affect the morphology of the resultant TiO_2 nanostructure, which can include anatase,[35] rutile,[29,74,88] brookite,[104] and amorphous TiO_2,[100] but no systematic data is available. Current reported research results are compiled in Table 2. Meng *et al.*[104] reported that the structures of sodium titanate nanowires derived from brookite and anatase were similar, but the fraction of short Ti–O bonds in sodium titanate from brookite is larger than in sodium titanate from anatase. Yuan *et al.*[100] used amorphous TiO_2 as the starting material, and found that the particles re-crystallized to become non-tubular needle-shaped titania nanocrystals with no nanotubes in the product. Yao *et al.*[105] also found that it is essential that the starting material be a crystalline structure to synthesize TiO_2 nanotubes, which can be delaminated into single-layer sheets. Nian *et al.*[67] have reported that single-crystalline anatase nanorods with a specific crystal-elongation direction can be obtained by hydrothermal treatment of titanate nanotube suspensions in an acidic environment. They found that the local shrinkage of the tube walls to form anatase crystallites and the subsequent oriented attachment of the crystallites are the key steps of the tube-to-rod structure transformation. Using titanate nanosheets as the initial raw material to form titanate nanotubes can decrease the hydrothermal synthesis temperature.[106,107] The transformation even can be achieved at ambient temperature using a simple alkali and acid treatment.[108,109] It was reported that the conditions during the post-treatment affect the formation, crystalline structure and chemical composition of the product. These steps include acid washing,[61,64,110] post-calcination treatment,[63] hydrothermal post-treatment,[66] hydrogen peroxide treatment,[89] and ultrasonic treatment.[111] Khan *et al.*[89] prepared TiO_2 nanotubes with ultrahigh crystallinity by using titania nanotubes of poor crystallinity, that were treated by 2 wt % hydrogen peroxide aqueous solutions under refluxing conditions at 40 °C for 4 h. The ultrahigh crystalline TiO_2 nanotubes have a length of 500–700 nm with quite clean tubular surfaces. They are hollow with an outside diameter of 8 nm and inside diameter of 5 nm.

The concentration and type of base solution used in the hydrothermal process can affect the resultant morphology of one-dimensional titanate nanostructures. By varying the base concentration, nanowire arrays, flowers of nanosheets and nanotubes, and urchin-like nanostructures of nanowires and nanotubes can be sequentially fabricated.[108] If the NaOH concentration is higher than 6 M, hydrated $Na_2Ti_6O_{13}$ nanowire arrays with diameters of 20–90 nm and an aspect ratio of 1100–5000 are produced at suitable reaction temperatures. In 4 M NaOH solutions, micrometre-sized flowers of nanotubes and nanosheets were formed. Reactions in 2 M NaOH solutions induce the production of urchin-like structures with a size of *ca.* 10 μm that are composed of nanotubes and nanowires. The results show that the relation between growth speed and repulsion of neighboring particles, which greatly depends on base concentration, plays an important role in formation of the different morphologies. The high rate of crystallization will result in the formation of nanofibers rather than nanotubes. When KOH is used in place of NaOH, nanowires and nanorods can be easily formed instead of nanotubes. Bavykin *et al.*[112] reported that by using a mixture of NaOH and KOH as a base, nanotubes can be synthesized at a lower temperature (about 100 °C).

3.1.2 Synthesis mechanisms. Since the discovery of the transformation of raw TiO_2 into nanotubular titanates, several research groups have studied the mechanism of titanate nanotube formation by using both theoretical and experimental methods. Some researchers assumed that nanotubular morphology arises during post-hydrothermal acid washing,[20,35]

Table 2 Synthesis of one-dimensional single-crystalline Ti–O based nanostructures using different raw materials

Raw material	Synthesis conditions	Morphologies	Ref.
TiO_2 nanotubes	Hydrothermal treatment at 175 °C for 48 h with pH values of 5.6	Nanorods: about 20 × 120 nm.	67
Natural rutile sand	Hydrothermal treatment at 150 °C for 72 h	Nanofibers: length of tens of mm to more than 100 mm	74
Amorphous TiO_2	Hydrothermal treatment at 100–160 °C for 48 h	Nanofibers: non-tubular needle-shaped fibers, thickness of 5–30 nm and length of a few tens to several hundreds of micrometres	100
Brookite nanocrystallites	Hydrothermal treatment at 180 °C for more than 12 days	Nanowires: average diameter of 75 nm with lengths up to several micrometres	104
Titanate nanosheets	Colloidal hydrated $Ti_{0.91}O_2$ nanosheets are poured into NaOH aqueous solution for overnight under stirring.	Nanotubes: apparently with hollow core, straight or conical.	108

and the layered titanate is transformed into nanotubes with the gradual substitution of Na^+ with H^+ by being washed with HCl. But Zhang *et al.*[113] demonstrated that nanotubular sodium titanates can be obtained by washing with ethanol or acetone. So they think that the titanium oxide nanotube arises from the reaction of TiO_2 with NaOH aqueous solution. There is general agreement that the reaction proceeds through several stages and that during treatment with concentrated NaOH, some of the Ti–O–Ti bonds are broken, forming an intermediate product containing Ti–O–Na and Ti–OH, then leading to the formation of lamellar fragments that are the intermediate phase in the formation process of the nanotube materials.[20,114] The trititanate lamellar fragments can be folded into tubular structures by certain driving force and grow along the axis during hydrothermal process. With exchange of sodium ions by protons during acid washing, sodium titanate nanotubes were transformed into titanic acid nanotubes. In summary, the transformation starts with scrolled up trititanate sheets and ends with the emergence of TiO_2 anatase nanotubes driven by dehydration, and even annealing induced nanotubes to nanorods at a high temperature. The appearance of isolated nanosheets during hydrothermal process is crucial to the formation of nanotubes.

Zhang *et al.*[114] and Wu *et al.*[56] proposed schematic models for the formation mechanism of Ti–O nanotubes and nanowires, as shown in Fig. 3. The formation process for Ti–O nanostructures is simply described as follows. First, the three-dimensional raw anatase-phase TiO_2, reacts with the NaOH aqueous solution and forms a lamellar product. The lamellar trititanate product possesses a two-dimensional layered structure. The edges of the lamellar products typically have many atoms with dangling bonds, and possess enough energy to destabilize the two-dimensional structure. Subsequently, the lamellar TiO_2 bends to saturate these dangling bonds. The nanoscale tubular structure is then achieved by further rolling and one-dimensional nanotubes are formed. The driving force for the scrolling of the nanosheets into nanotubes is proposed to be either the asymmetrical chemical environment on the two opposite sides of the nanosheet or the internal stress arising in multilayered nanosheets from an imbalance in width occurring during crystallization. The driving force for the wrapping may be the asymmetry due to the preferential doping of these nanosheets with hydrogen together with asymmetric surface forces due to locally high surface energy. For this reason, the surface chemistry can induce sheet exfoliation upon formation of the two-dimensional solids.[55,68] Zhang *et al.*[114] considered that single surface layers experience an asymmetric chemical environment, due to the imbalance of H^+ or Na^+ ion concentration on the two opposite sides of a nanosheet, giving rise to excess surface energy and resulting in bending. Another reason for bending of the multilayered nanosheets is that mechanical tension arises during the process of dissolution/crystallization. The curving of multilayered nanosheets to nanotubes passes through a sequence of metastable states that are stabilized by the periodic potential in the nanosheet lattice. Under alkaline hydrothermal conditions, nanosheets can also be converted to nanobelts or nanowires instead of rolling into nanotubes at a higher temperature (above 180 °C) or when KOH is used in place of NaOH. As for nanobelts, due to the different growth habits of TiO_2 along different axes (the fastest growth rate is along the b axis) and the faster crystallization rate at high hydrothermal temperatures, the thickness of the nanosheets will exceed a specific value, where they become too rigid to bend.

3.2 Other synthetic methods

The preparation of TiO_2 nanotubes[115–117] and nanorods[118] by chemical templating usually involves the controlled sol–gel hydrolysis of solutions of titanium-containing compounds in the presence of templating agents, followed by the polymerization of TiO_2 in the self-assembled template molecules or the deposition of TiO_2 onto the surface of the template aggregates. However, these one-dimensional TiO_2 structures are composed of small TiO_2 nanoparticles and cannot produce single-crystalline Ti–O based nanocrystals. Few reports on producing one-dimensional single-crystalline TiO_2 by other methods, such as the sol–gel method,[30] the electrochemical method,[119] the molten salt method[88,120,121] or the microwave method,[122] as represented in

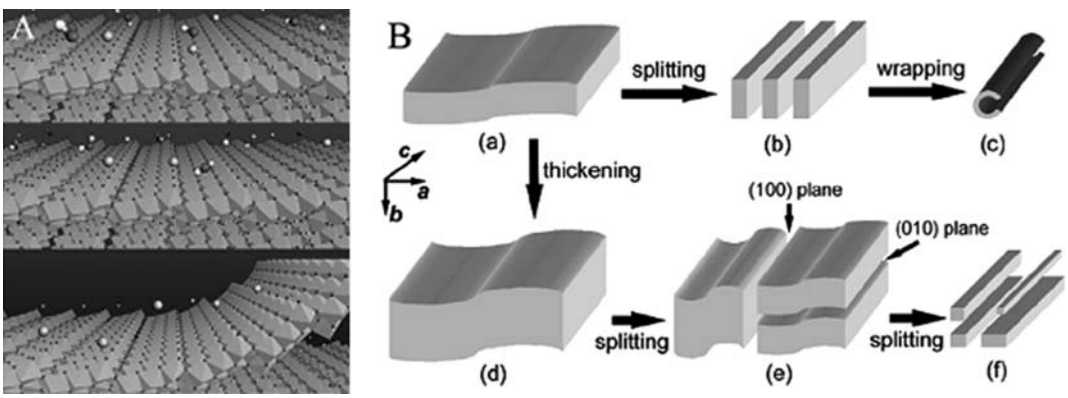

Fig. 3 Schematic drawings depicting the formation process of one-dimensional single-crystalline Ti–O based nanostructures: (A) schematic models showing the effect of the alkali environment and the cleavage of the surface layer due to hydrogen deficiency on the surface of $H_2Ti_3O_7$. White balls: H; black balls: O; gray balls: Na.[114] (B) schematic drawings depicting the formation process of $H_2Ti_3O_7$ nanotubes and nanowires: (a) Lamellar structures grown on the edges of TiO_2 particles. (b) Splitting of lamellar structures into nanosheets between (100) planes. (c) Wrapping of nanosheets into nanotubes; (d) Thick layers or wires formed after prolonged reaction at elevated temperature. (e) Splitting of these thick layers or wires between (100) and (010) planes. (d) Further splitting to form thin nanowires.[56]

Table 3 Other synthetic methods for producing one-dimensional single-crystalline Ti–O nanomaterials

Synthetic methods	Synthetic conditions	Morphologies	Ref.
Sol–gel	an unconstrained solution growth route by hydrolyzing TiF_4 under acidic conditions at 60 °C, anodic aluminium oxide (AAO) templates and Al_2O_3 nanoparticles as initial nucleation sites	TiO_2 nanotubes: the diameters of the inner tubes are 2.5–5 nm, the diameters of the outer tubes are 20–40 nm; lengths of up to a few hundred nanometres	30
Electrochemical method	cathodically induced sol–gel within the pores of an anodic aluminium oxide (AAO) template	TiO_2 nanowires: uniform diameter of about 40 nm; lengths of 2–10 μm	119
Molten salt method	one-step solid-state chemical reaction: KCl and TiO_2 nanoparticles as starting materials; then mixture is annealed at 950 °C for 3 h	$K_2Ti_6O_{13}$ nanobelts: 100–300 nm in diameter and 10–50 μm in length	121
Microwave method	KOH and TiO_2 mixed with alkali solution in PTFE vessel, reacting for 6 h microwave oven	$K_2Ti_6O_{13}$ nanowires: average diameter of about 10 nm and length ranging from hundreds of nanometres up to tens of micrometres	122

Table 3. Xu *et al.*[120] describe a simple method to synthesize single crystalline sodium titanate and potassium hollandite nanowires from reactions of TiO_2 nanoparticles with molten salt and NP-9 as a nonionic surfactant. The nanowires have a diameter of around 100 nm and a length of up to a few tens of microns. The synthesized sodium titanate and potassium hollandite nanowires were found to grow along the (010) and (001) crystal directions, respectively.

4. Modifications

As mentioned above, TiO_2 is a semiconductor with a wide band gap, and optical absorption in the UV region (<400 nm). Any highly efficient use of TiO_2 nanomaterials is sometimes prevented by the wide band gap. The band gap of bulk TiO_2 lies in the UV range (3.0 eV for the rutile phase and 3.2 eV for the anatase phase). Although TiO_2-based photocatalysts are very active in photocatalytic reactions, the major drawback delaying their widespread industrial use is the relatively short wavelength of light necessary for a photocatalytic reaction. Several approaches to sensitization of elongated titanate and TiO_2 nanostructures have recently been explored to reduce the band gap of TiO_2. Recently, assembling of quantum dots (Q-dots) on the TiO_2 surfaces to form heterojunctions has been investigated because of the potential applications in different fields, such as optoelectronics,[123] photocatalysis,[124] and biomedicine.[125] In addition to having a high surface-to-volume ratio, nanostructural TiO_2 in the form of nanotubes, nanowires, and nanobelts has advantages because it is more single-crystalline in nature when compared with nanoparticle titania, but there are few results reported. The match between the electronic structure of the excited nanomaterials and the TiO_2 basal body plays a large role in this process, as does the structure of the interface, including grain boundaries and bonding between the sensitizer and TiO_2. Careful design is needed to improve charge transfer and charge separation to avoid charge trapping and recombination.[126] There are several ways to achieve this goal. First, coupling the collective oscillations of the electrons in the conduction band of the metal nanoparticle surfaces to those in the conduction band of the TiO_2 nanomaterial in metal–TiO_2 nanocomposites can improve performance. Second, modification of the TiO_2 nanomaterial surface with other semiconductors can alter the charge-transfer properties between TiO_2 and the surrounding environment. As shown in Table 4, the nanomaterials used to modify one-dimensional single-crystalline Ti–O based nanomaterials include noble metals, such as Au,[39] Ag,[45] Pt,[127] Pd,[128] and semiconductors with narrow band gaps, such as ZnO,[38] CdS,[129,130] RuO_2,[131,132] V_2O_3.[133]

4.1 Metal Q-dots

Noble metals deposited on titania are known to induce strong metal-support interactions, which significantly affect the chemisorptive properties and catalytic reactions. The semiconductor–metal system produces a Schottky barrier at the interface, which can serve as an efficient electron trap, preventing electron–cavity recombination.[134] In the support role, a large surface area is the essential feature in order to disperse the active species. In addition, the microstructure or morphology of the support framework affects not only the dispersion but also the structure and chemical environment of the active species.[63]

Different metals have been attached to one-dimensional single-crystalline Ti–O based nanomaterials to form monodispersed metal nanoparticles, as shown in Fig. 4. Chien *et al.*[127] reported that immobilization of Pt and Au was carried out by a photochemical deposition method with TiO_2-nanotubes suspended in an aqueous solution containing $H_2PtCl_6 \cdot 6H_2O$ or $HAuCl_4 \cdot 3H_2O$. In general, Pt/TiO_2-nanotubes present a relatively higher activity than Au/TiO_2-nanotubes, and the catalytic activities of TiO_2 supported Pt and Au catalysts are significantly enhanced by the high surface area of the TiO_2-nanotube. Ma *et al.*[135] have reported that single crystalline Ag and Au nanoparticles with a narrow size distribution that correlates with the nanotubes have been obtained by treating the nanotubes with

Table 4 Different noble metals and semiconductors attached to one-dimensional single-crystalline Ti–O nanomaterials

Formula	Synthetic method	Morphologies	Performance	Ref.
Au/TNTs	Deposition–precipitation method	TiO_2 Nanotubes: uniform outer diameters of around 8–10 nm; inner diameter of around 6 nm; lengths range from several tens to several hundreds of nanometres. Au: about 5 nm nanoparticles	much higher WGS activity by 15–20% than that of a conventional Au/Al_2O_3	39
Ag/TNTs	Photoreduction method	TiO_2 Nanotubes: 250 nm long with a diameter of 20 nm Ag: about 20 nm nanoparticles	effective bactericidal activity at higher concentrations	45
Pd/TNTs	Reduction method	TiO_2 Nanotubes: outer diameter of about 15 nm and inner diameter of the nanotube of 10 nm Pd: 3wt (%)	better activity for methanol oxidation than that of TiO_2 nanoparticles and pure Pd	128
CdS/TNTs	Ion-exchange and precipitation method	TiO_2 Nanotubes: 150–200 nm long, 8–10 nm wide; hollow inner pore with open tube ends CdS: evenly distributed spherical CdS nanoparticles of about 6 nm	trititanate/CdS nanotube system active in photooxidation reaction	129
RuO_2/TNTs	Precipitation method	TiO_2 Nanotubes: outer diameter of 20–30 nm; inner diameter of 10–15 nm; length of about 1 μm. RuO_2: unobserved	good electrochemical capacitance performance (0–1.4V); high energy density of 12.5Wh/kg (150W kg^{-1}); good cycling performance(90%, 1000 cycles).	131
VOx/titanate-CNRs	Mix-Hydrothermal method	VOx/titanate-CNRs nanorods: length of 10 to 20 μm; diameter of 100 to 300 nm VOx: unobserved	better electrochemical capacitance performance than pure V_2O_5	133

$AgNO_3$ or $HAuCl_4$ aqueous solution followed by chemical reduction. The noble metal nanoparticles exhibit a strong surface plasmon absorption band. Multilayer film construction of the noble metal loaded nanotubes in a sequential layer-by-layer (LBL) assembly with polycations has also been achieved.

4.2 Semiconductor nanomaterials

The assembly of semiconductor Q-dots onto one-dimensional single-crystalline Ti–O based nanomaterials has been compiled in Fig. 5. Shen and co-workers[138,139] found more efficient electron diffusion in these single-crystalline nanomaterials. Using transition semiconductor Q-dots as the heterojunction alters the base material surface energy band structure, an effect that can improve optical properties, photocatalysis efficiency, and sensor performance. Among the Q-dots, cadmium-based semiconductors have been widely studied on titania electrodes. Kukovecz *et al.*[140] reported a novel synthetic route to prepare titanate nanotubes decorated with CdS nanoparticles *via* a complex-assisted process. With visible-light irradiation, the Q-dots inject electrons into the conduction band of TiO_2, generating a photocurrent and enhancing the photonductivity of titania. Chong *et al.*[141] reported that a nanocomposite consisting of 5 nm sized $CdS_{0.7}Se_{0.3}$ quantum dots hydrophobically attached to anatase TiO_2 nanobelts has been successfully prepared, with resulting enhancement in the photocurrent and good reproducibility. The TiO_2 nanobelts are able to accept electrons from the excited Q-dots and transport them to the TiO_2 surface to generate an anodic photocurrent. Apart from the alteration of electronic states by creating interfacial regions (such as p-n junctions), the organization pattern and shape of each component in an integrated nanocomposite further determines its ultimate physical and chemical properties and thus its performance. Yang *et al.*[38] reported that two important transition-metal-oxides, TiO_2 and ZnO, were sequentially grown onto the surface of the as-prepared nanobelts in aqueous mediums. Novel oxide nanocomposites of TiO_2 and ZnO with high structural complexity can be prepared in aqueous solutions. Currently, research on using anatase TiO_2 nanoparticle-coated one-dimensional TiO_2 nanocrystals has attracted a great deal of interest.[142,143] Zhu *et al.*[142] report on a delicate composite structure that consists of long titanate fibers of thickness 40–100 nm and length up to 30 μm long covered with anatase nanocrystals of 10–20 nm. It forms an interesting composite structure that possesses both the surface properties of the anatase nanocrystals and most of the morphological and mechanical properties of the titanate nanofibers. More importantly, this composite structure was achieved by the controlled reaction of titanate nanofibers with a dilute acid solution, and the titanate fibers were fabricated through a hydrothermal reaction of common inorganic titanium salt and a concentrated NaOH, rather than the conventional pyrolysis reaction above 827 °C.

5. Applications

Current and future applications of TiO_2 nanomaterials include paint, toothpaste, UV protection, photocatalysis, photovoltaics, sensors, and electrochromics and photochromic decices. These applications can be roughly divided into "energy" and "environmental" categories. TiO_2 nanomaterials normally have electronic band gaps larger than 3.0 eV and high absorption in the UV region. One-dimensional single-crystalline Ti–O based

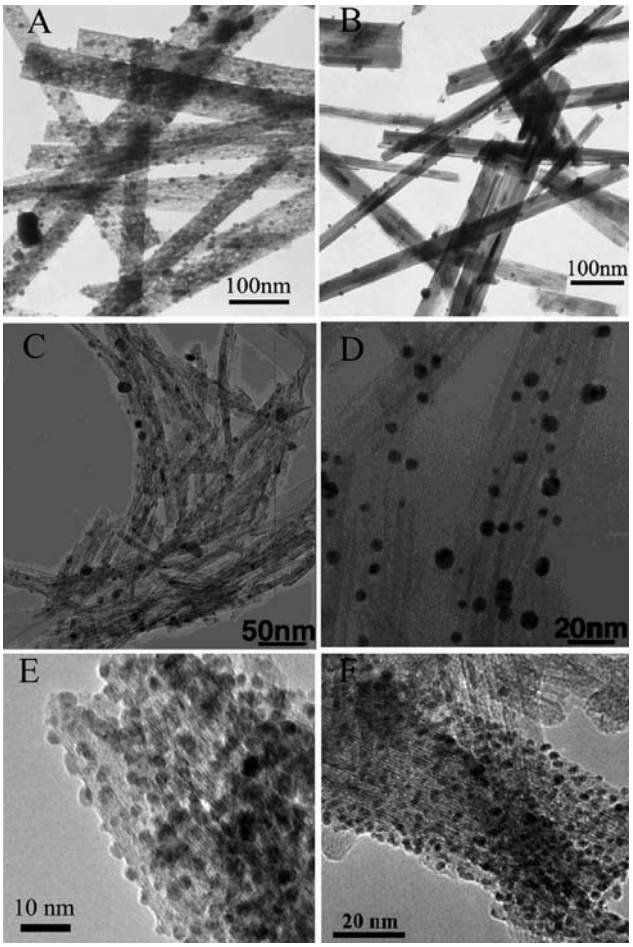

Fig. 4 Morphological properties of one-dimensional single-crystalline Ti–O based nanostructures modified by metals Q-dots. (A) Ag/mesoporous TiO_2 nanobelts and (B) $Ag/H_2Ti_3O_7$ nanobelts,[63] (C) Ag/TiO_2 nanotubes and (D) Au/TiO_2 nanotubes,[135] (E) Pd/TiO_2 nanotubes[136] and (F) Pt/TiO_2 nanotubes.[137]

nanostructures have a large surface area for the absorption of photons and provide channels for electron transfer. With these two characteristics, the performance of electronic devices, photocatalysts, and dye-sensitized solar cells (DSSCs) can be improved. Moreover, thin film nanoarrays composed of oriented nanotubes or nanowires can enhance the performance of current devices to expand the fields of application. From an energy or an environmental standpoint, one-dimensional Ti–O based nanomaterials has received attention due to its elongated morphology and its interesting physical and chemical properties, which lead to applications in photocatalysis,[23,144,145] lithium batteries,[146,147] sensors,[148,149] hydrogen production and storage,[150,151] solar cells[152,153] and biomedicine.[154]

5.1 Photocatalysts

TiO_2 is regarded as the most efficient and environmentally benign photocatalyst. The goal of research in this area is to look for efficient materials for photocatalytic processes, including the photocatalytic decomposition of various pollutants,[155–159] and killing bacteria.[40,160,161] The optical properties of one-dimensional titanates have been studied by various methods. During the last three decades, titanium dioxide has been comprehensively studied as a wide-band-gap photocatalyst. The principle of the semiconductor photocatalytic reaction is straightforward. Upon absorption of photons with energy larger than the band gap of TiO_2, electrons are excited from the valence band to the conduction band, creating electron–hole pairs. These charge carriers migrate to the surface and react with the chemicals adsorbed on the surface to decompose them. The increase in photocatalytic activity is induced by increasing the specific surface area,[109] the improvement of nanostructure crystallinity[89] and modifications of the metal and semiconductor Q-dots,[127,162] *etc*. Additional increase of the charge separation in titanate nanofibers or nanotubes can be achieved by using the recently discovered synergetic effect in mixed-phase nanocomposites

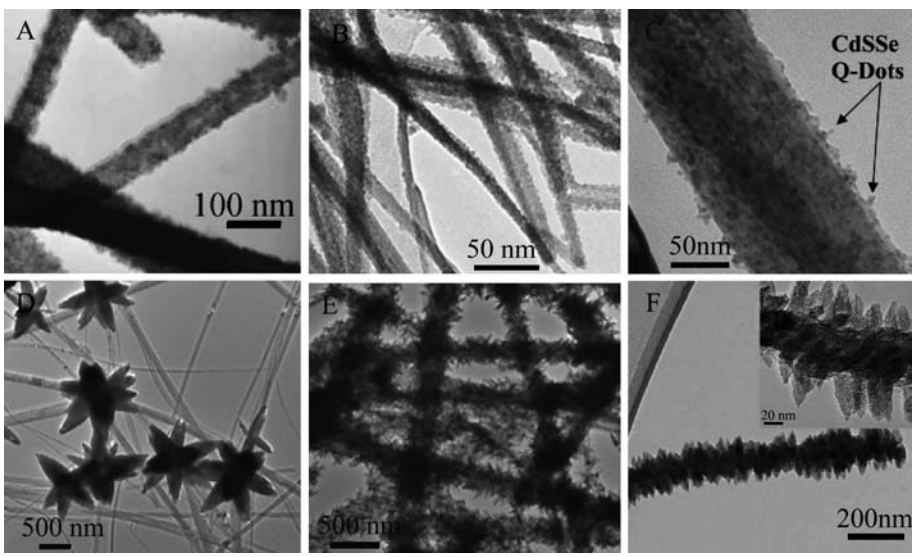

Fig. 5 Morphological properties of one-dimensional single-crystalline Ti–O based nanostructure modified by semiconductors with narrow band gaps. (A) CdS/TiO_2 nanowires,[129] (B) CdS/TiO_2 nanotubes,[140] (C) $CdSSe/TiO_2$ nanobelts,[141] (D) $ZnO/H_2Ti_5O_{11}\cdot H_2O$ nanobelts and (E) ZnO/TiO_2 nanobelts[38] and (F) TiO_2/titanate nanorods.[143]

occurring between two crystal forms of TiO_2 (anatase and rutile) due to the small difference in flat band potentials. This effect stimulates the spatial separation of carriers, reducing their recombination.[143,163,164] Ou *et al.*[165] reported that the photocatalytic activity of as-prepared titanate nanotubes was found to be smaller than the activity of the standard P25 catalyst in the oxidation of NH_3, which is a major nitrogen-containing pollutant in wastewater. This effect can be attributed either to sodium impurities or to the moderate crystallinity of the as-prepared titanate nanotubes.[166] A pure TNT phase presents no great ability to produce the photocatalytic reaction NH_3/NH_4^+, whereas the photocatalytic efficiency can be enhanced by the presence of a rutile phase within the TNTs. Hafez[110] found that nanorods obtained by acid treatment have a high BET surface of 85.06 $m^2\ g^{-1}$, which causes higher photocatalytic activity for the degradation of FN-R dye, compared with the results for titania nanoparticles and titanate nanotubes. TiO_2 nanotubes modified by RuO_2[132] and ruthenium(III) hydrated oxide[167] nanoparticles used as an electrocatalyst have a high activity for the reduction of CO_2 and the selective oxidation of alcohols. Dong *et al.*[168] reported on a new hydrothermal method for the synthesis of Ti–O based long nanowire catalysts that have been directly cast into a thermostable, robust, and multifunctional FSM-based 2D membrane structure of nearly any macroscopic size or shape. An immediate application of the long organized catalytic nanowire membranes is to produce a write–erase–rewrite function with the help of UV irradiation.

5.2 Lithium batteries

There has been increasing interest in developing one-dimensional nanostructure titanate electrode materials for application in rechargeable lithium batteries. Owing to their mesoporous structure, efficient transport of lithium ions, and good ion-exchange ratio, they exhibit a high charge/discharge capacity, good kinetic characteristics, and very good robustness and safety. These properties arise because the distance that Li^+ must diffuse is restricted to a value that is significantly smaller than that found in the typical powder fabricated electrode.[169–171] Alkaline ions diffuse along the length of the titanate nanotubes and nanofibers, which exhibit pseudocapacitive characteristic during the Li^+ insertion process. Moreover, the mixture of both the pseudocapacitive effect and the diffusion-limited reaction depends on different microstructures of the resulting samples.[172] Nanotubes and nanowires have an open layered structure with a much larger interlayer spacing, a feature that may make them promising candidates for lithium storage.[96] A notable change in the cathodic process between the first and second cycles displays large irreversible electrochemical discharge capacity of the as-prepared nanotubes calcined below 300 °C.

Recent studies[173,174] on the use of TiO_2 nanotubular anodes in a lithium battery demonstrate an initial 282 mA h g^{-1} discharge capacity at a specific current density of 0.24 mA g^{-1}. It is found that nanotubes calcined at 300 and 400 °C have larger surface areas and thus exhibit relatively larger reversible capacity and good reversibility (level remains at 200 mA h g^{-1} after 80 cycles).[172] Therefore, the fabrication of new materials with delicate 1D nanostructure is important for electrochemical lithium storage. Wang *et al.*[175] reported a new hybrid supercapacitor fabricated using 1D nanomaterials that consists of a carbon nanotube (CNT) cathode and a TiO_2(B) nanowire (TNW) anode. On the basis of the total weight of both active materials, the CNT–TNW supercapacitor delivers an energy density of 12.5 W h kg^{-1} at a rate of 10 C, double the value of the CNT–CNT supercapacitor, while maintaining desirable cycling stability. The anatase nanorods produced by calcination of TiNT are characterized by a lower discharge capacity, a characteristic plateau in the charge/discharge curve, and good reversibility.[176,177] Nanofibrous titanate materials have been more extensively studied than nanotubular ones for lithium-battery applications.[173,178] The cyclic V–I characteristic of titanate nanofibers shows several pairs of peaks in the voltage range from 1.5 to 2.0 V when compared to Li^+/Li. Bruce and co-workers[58] reported the formation of titanate nanowires and the conversion to TiO_2(B) nanowires by subsequent annealing. The TiO_2(B) electrode showed a very high specific charge storage capacity of 275 mA h/g and high rate capabilities for lithium intercalation by galvanostatic methods, which was much higher than that in normal TiO_2(B) electrodes and in nanostructured anatase.[173]

5.3 Sensor applications

TiO_2 nanomaterials have also been used as sensors for various gases and humidity by exploiting electrical or optical properties that change upon adsorption. Due to electrostatic effects between one-dimensional nanostructured TiO_2 and the anode surface, a practical approach for controlled deposition of nanostructured titanates on the surface of the electrodes is electrophoretic deposition of nanosheets[148] or nanorods[149] from aqueous suspension. Bavykin *et al.*[179] reported that TiO_2 nanotubes carry a stronger negative surface charge, under neutral conditions, providing electrostatic binding sites for cations. Compared with TiO_2 anatase nanoparticles, titanate nanotubes are excellent matrices for proteins to exhibit efficient direct reversible electron transfer and higher catalytic activity to hydrogen peroxide. The hydroxyl group, the surface charge and the tubular morphology of TNT play important roles in stabilizing the bound protein. Thus, TiO_2 nanotubes are novel, inert substrates that can be used for both inorganic and biological electrocatalysts. Liu *et al.*[180] reported that electrodes modified by a titanate-nanotube film provides a switch with an on/off function. The redox peak current of the Ti^{4+}/Ti^{3+} pair for a titanate-nanotube film-covered basal plane pyrolytic graphite disk electrode (PGE) was found to be sensitive to varying nitrate concentration in an acetate buffer solution. The TNT/PGE shows a stable redox peak in 0.1M acetate buffer that disappears when the same buffer solution contains over 5.6 mM of nitrate. The electrochemical activity of titanium oxide on the electrode surface can be reversibly repeated between the 0.1M acetate buffer solution (pH 5.5) and nitrate, just as with a switch have an on/off function. Wang *et al.*[160] prepared two-dimensional TiO_2 nanopapers from TiO_2 nanobelts using a paper-making process. The nanobelts are connected with hydrogen bonds and/or bridge oxygen atoms and packed together, forming a paperlike porous network structure. They demonstrated that sensitivity

of the nanostructured sheets to gas was present down to sub-ppb levels.

5.4 Hydrogen production and storage

Hydrogen is a favourite candidate for energy consumption, having high calorific value and producing only water on oxidation. The key to a hydrogen economy is a means to generate hydrogen efficiently and inexpensively on a renewable basis. When a semiconductor of proper characteristics is immersed in an aqueous electrolyte and irradiated with sunlight, sufficient energy is generated to split water into hydrogen and oxygen.[181] TiO_2 nanomaterials have been widely studied for water splitting and hydrogen production due to their suitable electronic band structure given the redox potential of water.[182–185] To maximize the hydrolytic efficiency of a TiO_2 photoanode, one would like to have a narrower band gap to utilize visible-light energy, and a high contact area with the electrolyte to increase the splitting of the e^-/h^+ pairs. Xu *et al.*[182] investigated the hydrolytic performance of carbon modified (CM)-n-TiO_2 nanotube arrays, and found about an eight-fold increase in photocurrent density in a carbon modified (CM)-n-TiO_2 nanotube film compared to that of an undoped n-TiO_2 flat thin film. Both the nanotube structure and carbon doping contributed to the enhancement of the photoresponse in the n-TiO_2. It was found that the bandgap of n-TiO_2 is reduced to 2.84 eV and an additional band is introduced in the gap at 1.30 eV above the valence band, which extends the utilization of solar energy including the visible and infrared regions.

However, successful implementation of the hydrogen economy in industry raises the challenge of the proper storage and transportation of hydrogen. A number of materials with nanotubular morphology have been studied as hydrogen adsorbents, including carbon nanotubes,[186] boron nitride[187] and MoS_2.[188] One-dimensional single-crystalline Ti–O based nanostructures are a good hydrogen adsorbent due to their high specific surface area and layered structure. Hydrogen can intercalate between layers in the walls of TiO_2 nanotubes forming the host–guest compounds $TiO_2 \cdot xH_2 (x \leq 1.5)$.[150] It can occupy interstitial cavities without chemical bonding. The OH groups in the nanotube lattice stabilize the hydrogen molecules with the weak van der Waals interaction. Kinetic studies of the intercalation of molecular hydrogen support the hypothesis that diffusion of hydrogen molecules in the axial direction between the layers in the multilayered walls of TiO_2 nanotubes is the rate-limiting step of the process of intercalation. From a proposed diffusion model, the rate of hydrogen intercalation depends on the inverse square of nanotube length. Bavykin[150] and Lim[151] found that temperature plays an important role in stored hydrogen capacity and steady-state. TiO_2 nanotubes can reproducibly store up to approximately 2 wt % H_2 at room temperature and at 6 MPa. This stored hydrogen is released when the pressure is lowered to ambient conditions due to physisorption.

5.5 Solar cells

When sensitized with organic dyes or inorganic narrow band gap semiconductors, TiO_2 can absorb light into the visible region and convert solar energy into electrical energy for solar cell applications. One-dimensional TiO_2 nanostructures have also been examined as excellent electrodes for dye-sensitized solar cells (DSSCs). One possible way to improve the diffusion coefficient and transport properties is to grow the electrode materials as one-dimensional nanostructures such as nanotubes and nanorods,[15] nanowires[189] and nanofibers.[190] The electrons are conducted to the outer circuit to drive the load and make electric power. The voltage generated under illumination corresponds to the difference between the Fermi level of TiO_2 and the redox potential of the electrolyte. An alternative way to achieve immobilization of one-dimensional titanates is to use direct alkaline hydrothermal synthesis on the surface of Ti metal.[95,191,192]

The potential advantage of titanate nanotubes as electrodes for DSSCs can be realized by utilizing the better adsorption of the positively charged dyes from aqueous solution on the surface of a negatively charged titanate nanotube, allowing a compact monolayer of dye to be deposited with a capacity of over 1000 molecules per nanotube. The second advantage of nanotubes is their one-dimensional morphology, which can provide a direct pathway for electron transfer from the point of injection to the electron sink with improved electron transport and a higher charge collection efficiency. Ohsaki *et al.*[86] and Adachi *et al.*[193] found that the higher efficiency of solar cells with single-crystalline TiO_2 nanotube-based electrodes results from an increase in electron density in the nanotube electrodes compared to the P25 electrodes. They found that the highly ordered TiO_2 nanotube arrays had superior electron lifetimes and provided excellent pathways for electron percolation by comparison to nanoparticulate systems. The use of TiO_2 nanowires may provide channels for fast electron transfer. A photoconversion efficiency above 9.3% has been reported for DSSCs using single crystal like anatase nanowires.[194] The TiO_2 nanoarray film was transferred to a transparent conductive glass substrate and used as a photoanode for a dye-sensitized solar cell.[195] A light-to-energy conversion efficiency of 6.58% for the DSSCs was obtained. Hence, Jsc and Z have been increased remarkably.

5.6 Biomedical applications

Because of the moderate electroconductivity, high surface area and affinity towards positively charged ions in aqueous solution, one-dimensional nanostructured titanates have recently been studied for possible applications to controlled drug delivery, labelling of biological objects and building of artificial tissues.[196] It has been reported that the redox mediator Meldola blue[181] and such oxygen transport metaloproteins as haemoglobin[197] or myoglobin[198] can be easily immobilized on the surface of TNTs, providing an efficient electron transfer facility between biological molecules and an artificial electrode. The main obstacle is the poor compatibility between inorganic materials and biomolecules. Titanium has a lower level of cell irritation than ceramic and gold, shows high biocompatibility and has been used in the fields of orthopedics and dentistry. There is significant interest in the development of technologies that modify the Ti surface for improving the interaction between bone cells and metal to improve bone cell materials and antimicrobial activities. The Ti surface can be modified by titania nanotubes[199] and nanofibers[154] to enhance bone–cell materials interactions, by providing rigidity

and a large macroporous structure suitable for cell growth and nutrition. The *in vitro* endothelial response of primary bovine aortic endothelial cells (BAECs) was investigated on a flat Ti surface *vs.* a nanostructured TiO_2 nanotube surface.[199] The nanotopography provided nanoscale cues that facilitated cellular probing, cell sensing, and especially cell migration, where more organized actin cytoskeletal filaments formed lamellipodia and locomotive morphologies. Sasaki *et al.*[200] implanted TiO_2 nanotubes with high biocompatibility under the inguinal skin of a nude mouse to analyze the biocompatibility and O_2 generation of TiO_2 nanotubes *via* the photodecomposition of water into O_2 and H_2 *in vivo*. Four weeks after the implantation, venous oxygen saturation (SvO_2) of the inguinal skin in the groups with TiO_2 nanotubes was 30–40% higher than that in the control group (54%). These findings indicate excellent biocompatibility and O_2 generation by TiO_2 nanotubes *in vivo*.

5.7 Other applications

There is a range of recent studies suggesting other possible applications of one-dimensional single-crystalline Ti–O nanomaterials. Wide-band gap semiconductor nanotubes have potential use as components in electronic and optical devices because of their transparency and high carrier excitation energy.[201,202] At the same time, TiO_2 nanomaterials have been widely explored as electrochromic devices, such as in electrochromic windows and displays. The color change of titanate nanotubes is more striking than that of TiO_2 nanoparticles. The significant electrochromism of the titanate nanotube is attributed to its layered nanostructure.[203] Recent interest in room-temperature ferromagnetic semiconductors and magnetic nanosized materials having a high aspect ratio has stimulated research into the synthesis and characterization of one-dimensional titanates and TiO_2 magnetic nanomaterials. Pure one-dimensional titanates have paramagnetic properties.[204] However, through doping with Co^{2+},[205] Fe^{3+}[206] and depositing nickel nanoparticles,[207] ferromagnetism results, providing for the possibility of new applications.

6. Summary

Over recent decades, the tremendous effort invested in TiO_2 nanomaterials has resulted in a large amount of data on their synthesis, properties, modifications and applications. One-dimensional single-crystalline titanates (nanotubes, nanobelts, nanowires and nanorods) due to their specific structure, possess a unique combination of physical and chemical properties (high specific surface area, efficient ion-exchange and electroconductivity) that provide a wide variety of possible applications. The one-dimensional single-crystalline titanates produced by the alkaline hydrothermal method have been thoroughly studied. However, the experimental parameters and the mechanism of transformation have prompted several unanswered questions: what is the effect of starting materials on nanostructure morphology? What is the precise structure of the nanotubes and the universal mechanism of transformation of layered nanosheets into nanotubes?. All of these issues need be systematically researched.

Modifications of one-dimensional single-crystalline Ti–O based nanomaterials are targets for further investigation. There is currently a gap in our knowledge about how permanent their properties are for different applications. Continuing breakthroughs in the modification of one-dimensional TiO_2 nanomaterials have revealed new properties and new applications with improved performance. The modifications include the addition of metal Q-dots and semiconductor nanomaterials to one-dimensional single-crystalline Ti–O based nanomaterials.

In this report, we have identified some of the promising applications of nanostructured titanate materials including photocatalysis, lithium batteries, sensor applications, hydrogen production and storage, *etc*. The applications of one-dimensional single-crystalline Ti–O based nanomaterials have been extensively researched with regard to their specific structure and properties. Future growth of research interest in one-dimensional single-crystalline Ti–O nanomaterials is anticipated in the areas of (1) improving on a unified synthesis mechanism and guiding large-scale synthesis of one-dimensional single-crystals, (2) modification of one-dimensional single-crystalline Ti–O based nanomaterials with improved performance revealing new properties and new applications, (3) biomedical applications including biosensors, biocompatible coatings and nanotubular drug delivery systems, (4) formation of 2D and 3D nanodevices from 1D single-crystalline Ti–O nanomaterials.

Acknowledgements

This research was supported by NSFC (Nos: 50872070, NSFDYS: 50925205, IRG, 50721002), and the Program of Introducing Talents of Discipline to Universities in China (111 program).

References

1 S. Iijima, *Nature*, 1991, **354**, 56–58.
2 B. Liu and H. C. Zeng, *J. Phys. Chem. B*, 2004, **108**, 5867–5874.
3 G. T. Chandrappa, N. Steunou, S. Cassaignon, C. Bauvais and J. Livage, *Catal. Today*, 2003, **78**, 85–89.
4 L. Xu, Y. Su, S. Li, Y. Q. Chen, Q. T. Zhou and S. Y. Feng, *J. Phys. Chem. B*, 2007, **111**, 760–766.
5 X. Xiang, C. Cao, Y. Guo and H. S. Zhu, *Chem. Phys. Lett.*, 2003, **378**, 660–664.
6 R. S. Yang and Z. L. Wang, *J. Am. Chem. Soc.*, 2006, **128**, 1466–1467.
7 M. Law, L. E. Greene and A. Radenovic, *J. Phys. Chem. B*, 2006, **110**, 22652–22663.
8 N. H. Zhao, G. J. Wang, Y. Huang, B. Wang, B. D. Yao and Y. P. Wu, *Chem. Mater.*, 2008, **20**, 2612–2614.
9 D. W. Kim, I. S. Hwang and S. J. Kwon, *Nano Lett.*, 2007, **7**, 3041–3045.
10 C. L. Yan and D. Xue, *J. Phys. Chem. B*, 2006, **110**, 25850–25855.
11 E. Reck and S. Seymour, *Macromol. Symp.*, 2002, **187**, 707–718.
12 S. A. Yuan, W. H. Chen and S. S. Hu, *Mater. Sci. Eng., C*, 2005, **25**, 479–485.
13 M. Zlamal, J. M. Macak, P. Schmuki and J. Krýsa, *Electrochem. Commun.*, 2007, **9**, 2822–2826.
14 P. D. Cozzoli, A. Kornowski and H. Weller, *J. Am. Chem. Soc.*, 2003, **125**, 14539–14548.
15 G. K. Mor, O. K. Varghese, M. Paulose, K. Shankar and C. A. Grimes, *Sol. Energy Mater. Sol. Cells*, 2006, **90**, 2011–2075.
16 M. Grätzel, *MRS Bull.*, 2005, **30**, 23–27.
17 I. A. Al-Homoudi, J. S. Thakur, R. Naik, G. W. Auner and G. Newaz, *Appl. Surf. Sci.*, 2007, **253**, 8607–8614.

18 A. Wisitsoraat, A. Tuantranont, E. Comini, G. Sberveglieri and W. Wlodarski, *IEEE Sens. 2005, [IEEE Conf. Sens.], 4th*, 2005, 1184–1187.
19 G. K. Mor, M. A. Carvalho, O. K. Varghese, M. V. Pishko and C. A. Grimes, *J. Mater. Res.*, 2004, **19**, 628–634.
20 C. C. Tsai and H. Teng, *Chem. Mater.*, 2006, **18**, 367–373.
21 J. Wang, D. N. Tafen, J. P. Lewis, Z. L. Hong, A. Manivannan, M. J. Zhi, M. Li and N. Q. Wu, *J. Am. Chem. Soc.*, 2009, **131**, 12290–12297.
22 Y. Lin, G. S. Wu, X. Y. Yuan, T. Xie and L. D. Zhang, *J. Phys.: Condens. Matter*, 2003, **15**, 2917–2922.
23 J. Joo, S. G. Kwon, T. Yu and M. Cho, *J. Phys. Chem. B*, 2005, **109**, 15297–15302.
24 C. Burda, X. Chen, R. Narayanan and M. A. El-Sayed, *Chem. Rev.*, 2005, **105**, 1025–1102.
25 D. S. Seo, H. Kim and J. K. Lee, *J. Cryst. Growth*, 2005, **275**, e2371–e2376.
26 G. H. Du, Q. Chen, P. D. Han, Y. Yu and L. M. Peng, *Phys. Rev. B: Condens. Matter Mater. Phys.*, 2003, **67**, 035323.
27 R. Z. Ma, Y. Bando and T. Sasaki, *Chem. Phys. Lett.*, 2003, **380**, 577–582.
28 Q. Chen, W. Zhou, G. Du and L. M. Peng, *Adv. Mater.*, 2002, **14**, 1208–1211.
29 Y. Lan, X. Gao, H. Zhu, Z. Zheng, T. Yan, F. Wu, S. P. Ringer and D. Song, *Adv. Funct. Mater.*, 2005, **15**, 1310–1318.
30 S. M. Liu, L. M. Gan, L. H. Liu, W. D. Zhang and H. C. Zeng, *Chem. Mater.*, 2002, **14**, 1391–1397.
31 T. Suzuki, Y. C. Tateishi, T. Sugimoto, S. Shinkai and K. Sada, *Sci. Technol. Adv. Mater.*, 2006, **7**, 605–608.
32 X. H. Li, W. M. Liu and H. L. Li, *Appl. Phys. A: Mater. Sci. Process.*, 2005, **80**, 317–320.
33 L. V. Taveira, J. M. Macak, H. L. Tsuchiya, F. P. Dick and P. Schmuki, *J. Electrochem. Soc.*, 2005, **152**, B405–410.
34 S. P. Albu, A. Ghicov, S. Aldabergenova, P. Drechsel, D. LeClere, G. E. Thompson, J. M. Macak and P. Schmuki, *Adv. Mater.*, 2008, **20**, 4135–4139.
35 T. Kasuga, M. Hiramatsu, A. Hoson, T. Sekino and K. Niihara, *Langmuir*, 1998, **14**, 3160–3163.
36 J. C. Kim, J. Choi, Y. B. Lee, J. H. Hong, J. I. Lee, J. W. Yang, W. I. Lee and N. H. Hur, *Chem. Commun.*, 2006, 5024–5026.
37 J. Qu, X. Zhang, Y. Wang and C. Xie, *Electrochim. Acta*, 2005, **50**, 3576–3580.
38 H. G. Yang and H. C. Zeng, *J. Am. Chem. Soc.*, 2005, **127**, 270–278.
39 V. Idakiev, Z. Y. Yuan, T. Tabakova and B. L. Su, *Appl. Catal., A*, 2005, **281**, 149–155.
40 D. Guin, S. V. Manorama, J. N. L. Latha and S. Singh, *J. Phys. Chem. C*, 2007, **111**, 13393–13397.
41 U. Diebold, *Surf. Sci. Rep.*, 2003, **48**, 53–229.
42 X. B. Chen and S. S. Mao, *Chem. Rev.*, 2007, **107**, 2891–2959.
43 A. Fujishima, X. X. Zhang and D. A. Trykc, *Surf. Sci. Rep.*, 2008, **63**, 515–582.
44 G. R. Patzke, F. Krumeich and R. Nesper, *Angew. Chem., Int. Ed.*, 2002, **41**, 2446–2461.
45 Y. Xia, P. Yang, Y. Sun, Y. Wu, B. Mayers, B. Gates, Y. Yin, F. Kim and H. Yan, *Adv. Mater.*, 2003, **15**, 353–389.
46 R. Z. Ma, K. Fukuda, T. Sasaki, M. Osada and Y. Bando, *J. Phys. Chem. B*, 2005, **109**, 6210–6214.
47 T. Kubo and A. Nakahira, *J. Phys. Chem. C*, 2008, **112**, 1658–1662.
48 R. E. Schaak and T. E. Mallouk, *Chem. Mater.*, 2002, **14**, 1455–1471.
49 Q. Chen, G. H. Du, S. Zhang and L. M. Peng, *Acta Crystallogr., Sect. B: Struct. Sci.*, 2002, **58**, 587–593.
50 X. M. Sun and Y. D. Li, *Chem.–Eur. J.*, 2003, **9**, 2229–2238.
51 J. Yang, Z. Jin, X. Wang, W. Li, J. Zhang, S. Zhang, X. Guo and J. Zhang, *Dalton Trans.*, 2003, 3898–3901.
52 A. Nakahira, W. Kato, M. Tamai, T. Isshiki, K. Nishio and H. Aritani, *J. Mater. Sci.*, 2004, **39**, 4239–4245.
53 D. N. Tafen and J. P. Lewis, *Phys. Rev. B: Condens. Matter Mater. Phys.*, 2009, **80**, 014104.
54 D. V. Bavykin, J. M. Friedrich and F. C. Walsh, *Adv. Mater.*, 2006, **18**, 2807–2824.
55 Z. V. Saponjic, N. M. Dimitrijevic, D. M. Tiede, A. J. Goshe, X. Zuo, L. X. Chen, A. S. Barnard, P. Zapol, L. Curtiss and T. Rajh, *Adv. Mater.*, 2005, **17**, 965–971.
56 D. Wu, J. Liu, X. N. Zhao, A. D. Li, Y. F. Chen and N. B. Ming, *Chem. Mater.*, 2006, **18**, 547–553.
57 G. Wang, Q. Wang, W. Lu and J. H. Li, *J. Phys. Chem. B*, 2006, **110**, 22029–22034.
58 A. R. Armstrong, G. Armstrong, J. Canales and P. G. Bruce, *Angew. Chem., Int. Ed.*, 2004, **43**, 2286–2288.
59 R. Beranek, H. Tsuchiya, T. Sugishima, J. M. Macak, L. Taveira, S. Fujimoto, H. Kisch and P. Schmuki, *Appl. Phys. Lett.*, 2005, **87**, 243114–243116.
60 C. W. Guo, Y. Cao, W. L. Dai and K. N. Fan, *Chem. Lett.*, 2002, 588–589.
61 C. C. Tsai and H. Teng, *Chem. Mater.*, 2004, **16**, 4352–4358.
62 A. Riss, M. J. Elser, J. Bernardi and O. Diwald, *J. Am. Chem. Soc.*, 2009, **131**, 6198–6206.
63 D. A. Wang, F. Zhou, C. W. Wang and W. Liu, *Microporous Mesoporous Mater.*, 2008, **116**, 658–664.
64 Y. Yu and D. Xu, *Appl. Catal., B*, 2007, **73**, 166–171.
65 P. Umek, P. Cevc, A. Jesih, A. Gloter, C. P. Ewels and D. Arčon, *Chem. Mater.*, 2005, **17**, 5945–5950.
66 H. G. Yu, J. G. Yu, B. Cheng and M. H. Zhou, *J. Solid State Chem.*, 2006, **179**, 349–354.
67 J. N. Nian and H. Teng, *J. Phys. Chem. B*, 2006, **110**, 4193–4198.
68 Y. B. Mao and S. S. Wong, *J. Am. Chem. Soc.*, 2006, **128**, 8217–8226.
69 N. Wang, H. Lin and J. B. Li, *J. Am. Ceram. Soc.*, 2006, **89**, 3564–3566.
70 D. V. Bavykin, J. M. Friedrich, A. A. Lapkin and P. K. Plucinski, *Chem. Mater.*, 2006, **18**, 1124–1129.
71 D. V. Bavykin, V. N. Parmon, A. A. Lapkin and F. C. Walsh, *J. Mater. Chem.*, 2004, **14**, 3370–3377.
72 E. Morgado Jr, P. M. Jardim, B. A. Marinkovic, F. C. Rizzo, M. A. S. de Abreu, J. L. Zotin and A. S. Araújo, *Nanotechnol.*, 2007, **18**, 495710.
73 A. Thorne, A. Kruth, D. Tunstall, J. T. S. Irvine and W. Zhou, *J. Phys. Chem. B*, 2005, **109**, 5439–5444.
74 S. Pavasupree, Y. Suzuki, S. Yoshikawa and R. Kawahata, *J. Solid State Chem.*, 2005, **178**, 3110–3116.
75 J. Suetake, A. Y. Nosaka, K. Hodouchi, H. Matsubara and Y. Nosaka, *J. Phys. Chem. C*, 2008, **112**, 18474–18482.
76 M. Qamar, C. R. Yoon, H. J. Oh, D. H. Kim, J. H. Jho, K. S. Lee, W. J. Lee, H. G. Lee and S. J. Kim, *Nanotechnology*, 2006, **17**, 5922–5929.
77 Y. V. Koleńko, K. A. Kovnir, A. I. Gavrilov and A. V. Garshev, *J. Phys. Chem. B*, 2006, **110**, 4030–4038.
78 O. P. Ferreira, A. G. Souza-Filho, J. Mendes-Filho and E. J. G. Santos, *J. Braz. Chem. Soc.*, 2006, **17**, 393–402.
79 R. Ma, T. Sasaki and Y. Bando, *Chem. Commun.*, 2005, 948–950.
80 J. Kim and J. Cho, *Electrochem. Solid-State Lett.*, 2007, **10**, A81–A84.
81 N. T. Q. Hoa, Z. Lee, S. H. Kang, V. Radmilovic and E. T. Kim1, *Appl. Phys. Lett.*, 2008, **92**, 122508.
82 H. Y. Zhang, T. H. Ji, L. L. Li, X. Y. Qi, Y. F. Liu and J. W. Cai, *Acta Phys.-Chim. Sin.*, 2008, **24**, 607–611.
83 D. V. Bavykin, S. N. Gordeev, A. V. Moskalenko, A. A. Lapkin and F. C. Walsh, *J. Phys. Chem. B*, 2005, **109**, 8565–8569.
84 N. Sakai, Y. Ebina, K. Takada and T. Sasaki, *J. Am. Chem. Soc.*, 2004, **126**, 5851–5858.
85 Y. X. Zhang, G. H. Li, Y. X. Jin, Y. Zhang and L. D. Zhang, *Chem. Phys. Lett.*, 2002, **365**, 300–304.
86 Y. Ohsaki, N. Masaki, T. Kitamura, Y. Wada and T. Okamoto, *Phys. Chem. Chem. Phys.*, 2005, **7**, 4157–4163.
87 L. Zhen, C. Y. Xu and W. S. Wang, *Appl. Surf. Sci.*, 2009, **255**, 4149–4152.
88 T. Kasuga, M. Hiramatsu, A. Hoson, M. Hirano and K. Oyamada, *Adv. Mater.*, 1999, **11**, 1307–1311.
89 M. A. Khan, H. T. Jung and O. Yang, *J. Phys. Chem. B*, 2006, **110**, 6626–6630.
90 L. Q. Weng, S. H. Song and S. Hodgson, *J. Eur. Ceram. Soc.*, 2006, **26**, 1405–1409.
91 X. M. Sun, X. Chen and Y. Li, *Inorg. Chem.*, 2002, **41**, 4996–4998.
92 E. Horváth, Á. Kukovecz, Z. Kónya and I. Kiricsi, *Chem. Mater.*, 2007, **19**, 927–931.
93 R. A. Zarate, S. Fuentes, A. L. Cabrera and V. M. Fuenzalida, *J. Cryst. Growth*, 2008, **310**, 3630–3637.
94 V. Stengl, S. Bakardjieva, J. Subrt, E. Vecernikova, L. Szatmary, M. Klementova and V. Balek, *Appl. Catal., B*, 2006, **63**, 20–30.

95 Z. R. R. Tian, J. A. Voigt, J. Liu, B. Mckenzie and H. F. Xu, *J. Am. Chem. Soc.*, 2003, **125**, 12384–12385.
96 M. Adachi, Y. Murata and S. Yoshikawa, *Chem. Lett.*, 2000, 942–943.
97 J. R. Li, Z. L. Tang and Z. T. Zhang, *Chem. Mater.*, 2005, **17**, 5848–5855.
98 A. Elsanousi, E. M. Elssfah, J. Zhang, J. Lin, H. S. Song and C. Tang, *J. Phys. Chem. C*, 2007, **111**, 14353–14357.
99 E. Morgado, M. A. S. de Abreu, G. T. Moure, B. A. Marinkovic, P. M. Jardim and A. S. Araujo, *Chem. Mater.*, 2007, **19**, 665–676.
100 Z. Y. Yuan and B. L. Su, *Colloids Surf., A*, 2004, **241**, 173–183.
101 H. H. Ou, S. L. Lo and Y. H. Liou, *Nanotechnology*, 2007, **18**, 175702–175706.
102 X. Wu, Q. Z. Jiang, Z. F. Ma, M. Fu and W. F. Shangguan, *Solid State Commun.*, 2007, **143**, 343–347.
103 Y. Ma, Y. Lin and X. Xiao, *Mater. Res. Bull.*, 2006, **41**, 237–243.
104 X. D. Meng, D. Z. Wang, J. H. Liu and S. Y. Zhang, *Mater. Res. Bull.*, 2004, **39**, 2163–2170.
105 B. D. Yao, Y. F. Chan, X. Y. Zhang, W. F. Zhang, Z. Y. Yang and N. Wang, *Appl. Phys. Lett.*, 2003, **82**, 281–283.
106 M. D. Wei, Y. Konishi, H. S. Zhou, H. Sugihara, H. Arakawa and M. Ichihara, *Solid State Commun.*, 2005, **133**, 493–497.
107 P. H. Wen, H. Itoh, W. P. Tang and Q. Feng, *Langmuir*, 2007, **23**, 11782–11790.
108 R. Ma, Y. Bando and T. Sasaki, *J. Phys. Chem. B*, 2004, **108**, 2115–2119.
109 C. C. Tsai and H. Teng, *Langmuir*, 2008, **24**, 3434–3438.
110 H. S. Hafez, *Mater. Lett.*, 2009, **63**, 1471–1474.
111 N. Viriyaempikul, N. Sano, T. Charinpanitkul, T. Kikuchi and W. Tanthapanichakoon, *Nanotechnology*, 2008, **19**, 35601–35606.
112 D. V. Bavykin, B. A. Cressey, M. E. Light and F. C. Walsh, *Nanotechnology*, 2008, **19**, 275604–275605.
113 M. Zhang, Z. S. Jin, J. W. Zhang, X. Y. Guo, J. J. Yang, W. Li, X. D. Wang and Z. J. Zhang, *J. Mol. Catal. A: Chem.*, 2004, **217**, 203–210.
114 S. Zhang, L. M. Peng, Q. Chen, G. H. Du, G. Dawson and W. Z. Zhou, *Phys. Rev. Lett.*, 2003, **91**, 256103.
115 M. S. Sander, M. J. Cote, W. Gu, B. M. Kile and C. P. Tripp, *Adv. Mater.*, 2004, **16**, 2052–2057.
116 S. I. Na, S. S. Kim, W. K. Hong, J. W. Park, J. Jo, Y. C. Nah, T. Lee and D. Y. Kim, *Electrochim. Acta*, 2008, **53**, 2560–2566.
117 M. Zhang, Y. Bando and K. Wada, *J. Mater. Sci. Lett.*, 2001, **20**, 167–170.
118 L. Miao, S. Tanemura, S. Toh, K. Kaneko and M. Tanemura, *J. Cryst. Growth*, 2004, **264**, 246–252.
119 Z. Miao, D. S. Xu, J. H. Ouyang, G. Guo, X. Zhao and Y. Tang, *Nano Lett.*, 2002, **2**, 717–720.
120 C. Y. Xu, Q. Zhang, H. Zhang, L. Zhen, J. Tang and L. C. Qin, *J. Am. Chem. Soc.*, 2005, **127**, 11584–11585.
121 X. K. Zhang, S. L. Tang, L. Zhai, J. Y. Yu, Y. G. Shi and Y. W. Du, *Mater. Lett.*, 2009, **63**, 887–889.
122 J. J. Zhang, Y. A. Wang, J. J. Yang, J. M. Chen and Z. J. Zhang, *Mater. Lett.*, 2006, **60**, 3015–3017.
123 T. Hirakawa and P. V. Kamat, *Langmuir*, 2004, **20**, 5645–5647.
124 H. Tada, T. Ishida, A. Takao and S. Ito, *Langmuir*, 2004, **20**, 7898–7900.
125 V. Alt, T. Bechert, P. Steinrücke, M. Wagener, P. Seidel, E. Dingeldein, E. Domann and R. Schnettler, *Biomaterials*, 2004, **25**, 4383–4391.
126 G. J. Meyer, *Inorg. Chem.*, 2005, **44**, 6852–6864.
127 S. H. Chien, Y. C. Liou and M. Kuo, *Synth. Met.*, 2005, **152**, 333–336.
128 M. Wang, D. J. Guo and H. L. Li, *J. Solid State Chem.*, 2005, **178**, 1996–2000.
129 J. Cao, J. Z. Sun, H. Y. Li, J. Hong and M. Wang, *J. Mater. Chem.*, 2004, **14**, 1203–1206.
130 M. Hodos, E. Horvath, H. Haspel, Á. Kukovecz, Z. Kónya and I. Kiricsi, *Chem. Phys. Lett.*, 2004, **399**, 512–515.
131 Y. G. Wang, Z. D. Wang and Y. Y. Xia, *Electrochim. Acta*, 2005, **50**, 5641–5646.
132 Y. G. Wang and X. G. Zhang, *Electrochim. Acta*, 2004, **49**, 1957–1962.
133 L. Yu and X. Zhang, *Mater. Chem. Phys.*, 2004, **87**, 168–172.
134 L. Chmielarz, P. trowski, M. Zbroja, A. Rafalskaasocha, B. Dudek and R. Dziembaj, *Appl. Catal., B*, 2003, **45**, 103–116.
135 R. Ma, T. Sasaki and Y. Bando, *J. Am. Chem. Soc.*, 2004, **126**, 10382–10388.
136 F. C. Walsh, D. V. Bavykin, L. Torrente-Murciano, A. A. Lapkin and B. A. Cressey, *Trans. Inst. Met.Finish.*, 2006, **84**, 293–299.
137 D. V. Bavykin, A. A. Lapkin, P. K. Plucinski, L. Torrente-Murciano, J. M. Friedrich and F. C. Walsh, *Top. Catal.*, 2006, **39**, 151–160.
138 Q. Shen, K. Katayama, T. Q. S. Sawada, K. Katayama, T. Sawada, M. Yamaguchi and T. Toyoda, *Jpn. J. Appl. Phys.*, 2006, **45**, 5569–5574.
139 Q. Shen, T. Sato, M. Hashimoto, C. Chen and T. Toyoda, *Thin Solid Films*, 2006, **499**, 299–305.
140 Á. Kukovecz, M. Hodos, Z. Kónya and I. Kiricsi, *Chem. Phys. Lett.*, 2005, **411**, 445–449.
141 S. V. Chong, N. Suresh, J. Xia, N. Al-Salim and H. Idriss, *J. Phys. Chem. C*, 2007, **111**, 10389–10393.
142 H. Y. Zhu, X. P. Gao, Y. Lan, D. Song, Y. Xi and J. Zhao, *J. Am. Chem. Soc.*, 2004, **126**, 8380–8381.
143 H. G. Yu, C. Bei and J. G. Yu, *J. Mol. Catal. A: Chem.*, 2006, **253**, 99–106.
144 G. K. Mor, K. Shankar, M. Paulose, O. K. Varghese and C. A. Grimes, *Nano Lett.*, 2005, **5**, 191–195.
145 S. Takabayashi, R. Nakamura and Y. Nakato, *J. Photochem. Photobiol., A*, 2004, **166**, 107–113.
146 C. R. Sides and C. R. Martin, *Adv. Mater.*, 2005, **17**, 125–128.
147 A. Zak, Y. Feldman, V. Lyakhovitskaya, G. Leitus, R. Popovitz-Biro, E. Wachtel, H. Cohen, S. Reich and R. Tenne, *J. Am. Chem. Soc.*, 2002, **124**, 4747–4758.
148 W. Sugimoto, O. Terabayashi, Y. Murakami and Y. Takasu, *J. Mater. Chem.*, 2002, **12**, 3814–3818.
149 G. Z. Cao, *J. Phys. Chem. B*, 2004, **108**, 19921–19931.
150 D. V. Bavykin, A. A. Lapkin, P. K. Plucinski, J. M. Friedrich and F. C. Walsh, *J. Phys. Chem. B*, 2005, **109**, 19422–19427.
151 S. H. Lim, J. Z. Luo, Z. Y. Zhong, W. Ji and J. Y. Lin, *Inorg. Chem.*, 2005, **44**, 4124–4126.
152 M. Grätzel, *J. Photochem. Photobiol., C*, 2003, **4**, 145–153.
153 C. G. Granqvist, *Adv. Mater.*, 2003, **15**, 1789–1803.
154 W. J. Dong, T. R. Zhang, J. Epstein, L. Cooney, H. Wang, Y. B. Li, Y. B. Jiang, A. Cogbill, V. Varadan and Z. R. Tian, *Chem. Mater.*, 2007, **19**, 4454–4459.
155 J. H. Park, S. Kim and A. J. Bard, *Nano Lett.*, 2006, **6**, 24–28.
156 F. B. Li, X. Z. Li and M. F. Hou, *Appl. Catal., B*, 2004, **48**, 185–194.
157 J. Yu, H. Yu, B. Cheng and C. Trapalis, *J. Mol. Catal. A: Chem.*, 2006, **249**, 135–142.
158 H. Zhou, T. J. Park and S. S. Wong, *J. Mater. Res.*, 2006, **21**, 2941–2947.
159 X. W. Zhang, J. H. Pan, A. J. Du, W. J. Fu, D. D. Sun and J. O. Leckie, *Water Res.*, 2009, **43**, 1179–1186.
160 Y. M. Wang, G. J. Du, H. Liu, D. Liu, S. B. Qin, N. Wang, C. G. Hu, X. T. Tao, J. Jiao, J. Y. Wang and Z. L. Wang, *Adv. Funct. Mater.*, 2008, **18**, 1131–1137.
161 N. M. Mahmoodi, M. Arami, N. Y. Limaee and N. S. Tabrizi, *Chem. Eng. J.*, 2005, **112**, 191–196.
162 J. S. Jang, S. H. Choi, D. H. Kim, J. W. Jang, K. S. Lee and J. S. Lee, *J. Phys. Chem. C*, 2009, **113**, 8990–8996.
163 H. G. Yu, J. G. Yu, B. Cheng and J. Lin, *J. Hazard. Mater.*, 2007, **147**, 581–587.
164 G. Li, S. Ciston, Z. V. Saponjic, L. Chen and N. M. Dimitrijevic, *J. Catal.*, 2008, **253**, 105–110.
165 H. H. Ou, C. H. Liao, Y. H. Liou, J. H. Hong and S. L. Lo, *Environ. Sci. Technol.*, 2008, **42**, 4507–4512.
166 X. Zhu, S. R. Castleberry, M. A. Nanny and E. C. Butler, *Environ. Sci. Technol.*, 2005, **39**, 3784–3791.
167 D. V. Bavykin, A. A. Lapkin, P. K. Plucinski, J. M. Friedrich and F. C. Walsh, *J. Catal.*, 2005, **235**, 10–17.
168 W. J. Dong, A. Cogbill, T. R. Zhang, S. Ghosh and Z. R. Tian, *J. Phys. Chem. B*, 2006, **110**, 16819–16822.
169 H. S. Zhou, D. L. Li, M. Hibino and I. Honma, *Angew. Chem., Int. Ed.*, 2005, **44**, 797–802.
170 J. W. Xu, C. H. Jia, B. Cao and W. F. Zhang, *Electrochim. Acta*, 2007, **52**, 8044–8047.

171 A. R. Armstrong, G. Armstrong, J. Canales and P. G. Bruce, *J. Power Sources*, 2005, **146**, 501–506.
172 H. Zhang, G. R. Li, L. P. An, T. Y. Yan, X. P. Gao and H. Y. Zhu, *J. Phys. Chem. C*, 2007, **111**, 6143–6148.
173 A. R. Armstrong, G. Armstrong, J. Canales, R. Garcia and P. G. Bruce, *Adv. Mater.*, 2005, **17**, 862–865.
174 X. Gao, H. Zhu, G. Pan, S. Ye, Y. Lan, F. Wu and D. Song, *J. Phys. Chem. B*, 2004, **108**, 2868–2872.
175 Q. Wang, Z. H. Wen and J. Li, *Adv. Funct. Mater.*, 2006, **16**, 2141–2146.
176 G. Armstrong, A. R. Armstrong, J. Canales and P. G. Bruce, *Chem. Commun.*, 2005, 2454–2456.
177 J. Li, Z. Tang and Z. Zhang, *Electrochem. Commun.*, 2005, **7**, 62–67.
178 L. Kavan, M. Kalbac, M. Zukalova, I. Exnar, V. Lorenzen, R. Nesper and M. Grätzel, *Chem. Mater.*, 2004, **16**, 477–485.
179 D. V. Bavykin, E. V. Milsom, F. Marken, D. H. Kim, D. H. Marsh, D. J. Riley, F. C. Walsh, K. H. El-Abiary and A. A. Lapkin, *Electrochem. Commun.*, 2005, **7**, 1050–1058.
180 A. H. Liu, H. S. Zhou, I. Honma and M. Ichihara, *Appl. Phys. Lett.*, 2007, **90**, 253112.
181 M. Ni, M. K. H. Leung, D. Y. C. Leung and K. Sumathy, *Renewable Sustainable Energy Rev.*, 2007, **11**, 401–425.
182 C. K. Xu, Y. A. Shaban, W. B. Ingler and S. Khan, *Sol. Energy Mater. Sol. Cells*, 2007, **91**, 938–943.
183 C. C. Tsai and H. Teng, *Appl. Surf. Sci.*, 2008, **254**, 4912–4918.
184 H. L. Kuo, C. Y. Kuo, C. H. Liu, J. H. Chao and C. H. Lin, *Catal. Lett.*, 2007, **113**, 7–12.
185 J. Jitputti, Y. Suzuki and S. Yoshikawa, *Catal. Commun.*, 2008, **9**, 1265–1271.
186 A. C. Dillon, K. M. Jones, T. A. Bekkedahl, C. H. Kiang, D. S. Bethune and M. J. Heben, *Nature*, 1997, **386**, 377–379.
187 R. Ma, Y. Bando and H. Zhu, *J. Am. Chem. Soc.*, 2002, **124**, 7672–7673.
188 J. Chen, S. L. Li and Z. L. Tao, *J. Alloys Comput.*, 2003, **413**, 356–357.
189 M. Adachi, J. Jiu and S. Isoda, *Curr. Nanosci.*, 2007, **3**, 285–295.
190 V. Thavasi, G. Singh and S. Ramakrishna, *Energy Environ. Sci.*, 2008, **1**, 205–221.
191 J. E. Boercker and E. Enache-Pommer, *Nanotechnology*, 2008, **19**, 095604(10pp).
192 M. Wei, Y. Konishi, H. Zhou, H. Sugihara and H. Arakawa, *J. Electrochem. Soc.*, 2006, **153**, A1232–1236.
193 M. Adachi, Y. Murata and I. Okada, *J. Electrochem. Soc.*, 2003, **150**, G488–488.
194 M. Adachi, Y. Murata, J. Takao, J. T. Jiu, M. Sakamoto and F. M. Wang, *J. Am. Ceram. Soc.*, 2004, **126**, 14943–14949.
195 W. L. Wang, H. Lin, J. B. Li and N. Wang, *J. Am. Ceram. Soc.*, 2008, **91**, 628–631.
196 W. J. Parak, D. Gerion, T. Pellegrino, Zanchet, C. Micheel, S. C. Williams, R. Boudreau, M. A. LeGros, C. A. Larabell and P. A. Alivisatos, *Nanotechnology*, 2003, **14**, R15–27.
197 W. Zheng, Y. F. Zheng, K. W. Jin and N. Wang, *Talanta*, 2008, **74**, 1414–1419.
198 A. Liu, M. Wei, I. Honma and H. S. Zhou, *Anal. Chem.*, 2005, **77**, 8068–8074.
199 K. S. Brammer, S. Oh, J. O. Gallagher and S. Jin, *Nano Lett.*, 2008, **8**, 786–793.
200 K. Sasaki, K. Asanuma, K. Johkura, T. Kasuga, Y. Okouchi, N. Ogiwara, S. Kubota, R. Teng, L. Cui and X. Zhao, *Ann. Anat.*, 2006, **188**, 137–142.
201 J. Goldberger, R. He, Y. Zhang, S. Lee, H. Yan, H. J. Choi and P. Yang, *Nature*, 2003, **422**, 599–602.
202 Y. Li, Y. Bando and D. Golberg, *Adv. Mater.*, 2003, **15**, 1294–1296.
203 H. Tokudome and M. Miyauchi, *Angew. Chem., Int. Ed.*, 2005, **44**, 1974–1977.
204 C. Huang, X. Liu and L. Kong, *Appl. Phys. A: Mater. Sci. Process.*, 2007, **87**, 781–786.
205 X. W. Wang, X. P. Gao and G. R. Li, *J. Phys. Chem. C*, 2008, **112**, 5384–5389.
206 X. G. Xu, X. Ding and Q. Chen, *Phys. Rev. B: Condens. Matter Mater. Phys.*, 2006, **73**, 165403–165405.
207 J. Jiang, Q. Gao and Z. Chen, *Mater. Lett.*, 2006, **60**, 3803–3808.

